

Revised value of the eighth-order electron $g-2$

T. Aoyama,¹ M. Hayakawa,² T. Kinoshita,³ and M. Nio¹

¹*Theoretical Physics Laboratory, Nishina Center, RIKEN, Wako, Saitama 351-0198, Japan*

²*Department of Physics, Nagoya University, Nagoya, Aichi 464-8602, Japan*

³*Newman Laboratory for Elementary-Particle Physics,
Cornell University, Ithaca, New York 14853, U.S.A.*

(Dated: February 1, 2008)

The contribution to the eighth-order anomalous magnetic moment ($g-2$) of the electron from a set of diagrams without closed lepton loops is recalculated using a new FORTRAN code generated by an automatic code generator. Comparing the contributions of individual diagrams of old and new calculations, we found an inconsistency in the old treatment of infrared subtraction terms in two diagrams. Correcting this error leads to the revised value $-1.9144 (35)(\alpha/\pi)^4$ for the eighth-order term. This theoretical change induces the shift of the inverse of the fine structure constant by $-6.41180(73) \times 10^{-7}$.

PACS numbers: 13.40.Em, 14.60.Cd, 12.20.Ds, 06.20.Jr

The anomalous magnetic moment ($g-2$) of the electron has played a central role in testing the validity of QED [1, 2]. Recently, a Harvard group measured the electron $g-2$ value [3] using a Penning Trap with a cylindrical cavity [4]. Their result for $a_e \equiv (g-2)/2$ [3]

$$a_e = 1\,159\,652\,180.85(0.76) \times 10^{-12} \quad [0.66\text{ppb}], \quad (1)$$

has a 5.5 times smaller uncertainty than the best previous measurement [5].

To match the precision of this measurement the theory of $g-2$ must include up to the eighth-order contribution of the QED perturbation theory [2, 6, 7, 8, 9, 10] as well as the hadronic [11, 12] and weak contributions [13]. The tenth-order contribution of QED $A_1^{(10)}(\alpha/\pi)^5$ might be relevant, but at present it is not known. As a temporary measure we adopt the bound $A_1^{(10)} = 0$ (3.8) proposed in Ref. [14] to indicate a likely range of value taken by $A_1^{(10)}$. This will soon be replaced by an actual number which is being evaluated right now [15, 16, 17]. Until then, the tenth-order term is the source of the largest theoretical uncertainty of the electron $g-2$. The next largest uncertainty comes from the numerical integration of the eighth-order coefficient $A_1^{(8)}$ [10].

The purpose of this letter is to report the new value

$$A_1^{(8)} = -1.914\,4 (35) \quad (2)$$

obtained by combining the information derived from the previous result [10] and a new and independent evaluation of $A_1^{(8)}$ by means of FORTRAN codes generated by an automatic code generator “gencodeN” [15, 16].

$A_1^{(8)}$ receives contributions from 891 Feynman diagrams. 373 of them that have closed lepton loops had been calculated by more than two independent methods [10]. The remaining 518 diagrams that have no closed lepton loop (called q -type) form one gauge invariant set (Group V). In our formulation these diagrams are repre-

sented by self-energy-like diagrams related by the Ward-Takahashi identity. Taking the time reversal symmetry of QED into account, 518 vertex diagrams are amalgamated into 47 self-energy-like diagrams shown in Fig. 1. Their integrands were carefully analyzed and checked by various means. However, no independent check of calculation has been attempted until now.

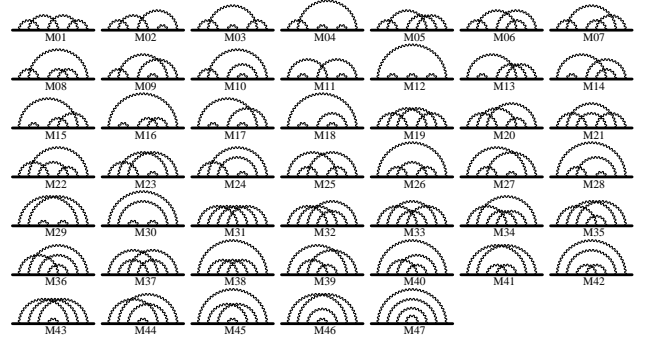


FIG. 1: Eighth-order Group V diagrams. 47 self-energy-like diagrams of $M_{01} - M_{47}$ represent 518 vertex diagrams.

Technical progress in handling UV- and IR-divergences has enabled us to generate the N th-order FORTRAN code easily and swiftly [15, 16]. Although “gencodeN” was developed primarily to handle the tenth-order term, we have applied it to fourth-, sixth- and eighth-order q -type diagrams as part of the debugging effort. With the help of “gencodeN” eighth-order codes are generated easily. However, their numerical evaluation by VEGAS [18] is quite nontrivial and requires huge computational resource. Numerical work has thus far reached relative uncertainty of about 3 %. Although this is more than an order of magnitude less accurate than the uncertainty of the old calculation [10], it is good enough for checking algebra of the old calculation.

Ultraviolet (UV) divergences of vertex and self-energy subdiagrams are removed by the K -operation [15, 19,

TABLE I: Comparison of the numerical calculation of $M_{01}-M_{24}$ of the eighth-order Group V diagrams. The second column shows the analytic expression of the difference of old and new calculations of the magnetic moment. The third column, value A , is obtained by plugging lower-order renormalization constants, such as $\Delta M_{4a}, \Delta L_{4s}$ into the expression in the second column. The fourth column, value B , lists the numerical values of $\Delta M^{\text{old}} - \Delta M^{\text{new}}$. The fifth column is the difference $A - B$. If both numerical calculations are correct, $A - B$ must vanish within the numerical uncertainty. In evaluating ΔM^{new} the double precision is used for the diagrams without a self-energy subdiagram, while the quadruple precision is used for the reminder.

Diagram	difference	value A	value B	$A - B$
M_{01}	0	0	-0.0129(47)	0.0129(47)
M_{02}	$2\Delta L_{6f1} M_2$	-0.0066(3)	0.0018(127)	-0.0084(127)
M_{03}	$\Delta L_{6f3} M_2$	-0.1132(2)	-0.1055(100)	-0.0076(100)
M_{04}	$2(\Delta L_{6d1} + \Delta L_{6d3}) M_2$	0.3338(6)	0.3515(221)	-0.0177(221)
M_{05}	0	0	0.0020(28)	-0.0020(28)
M_{06}	0	0	-0.0223(61)	0.0223(61)
M_{07}	0	0	-0.0102(40)	0.0102(40)
M_{08}	$2(\Delta \delta m_{4a} \Delta M_{4a(1^*)} + \Delta L_{4c} \Delta M_{4a})$	-2.1809(7)	-2.1773(163)	-0.0011(163)
M_{09}	$2\Delta L_{6f2} M_2$	0.0805(2)	0.0912(122)	-0.0106(122)
M_{10}	$2(\Delta \delta m_{4b} \Delta M_{4a(1^*)} + \Delta L_{6d2} M_2 + \Delta L_{4c} \Delta M_{4b})$	15.8899(49)	15.8615(210)	0.0284(216)
M_{11}	$2\Delta L_{6d5} M_2$	0.6948(3)	0.6827(112)	0.0121(112)
M_{12}	$2(\Delta L_{6a1} + \Delta L_{6a3}) M_2$	1.2841(0)	1.2875(74)	-0.0034(74)
M_{13}	$2\Delta L_{6h1} M_2$	-0.4202(4)	-0.4238(48)	0.0036(48)
M_{14}	$2\Delta L_{6g5} M_2$	0.0892(3)	0.0960(95)	-0.0068(95)
M_{15}	$2\Delta L_{6g1} M_2$	0.0889(3)	0.0893(71)	-0.0004(71)
M_{16}	$2(\Delta \delta m_{4a} \Delta M_{4b(1^*)} + \Delta L_{6c1} M_2 + \Delta L_{4s} \Delta M_{4a})$	-2.6042(6)	-2.6316(235)	0.0274(235)
M_{17}	$2(\Delta L_{6e1} + \Delta L_{6d4}) M_2$	-2.1183(5)	-2.1010(189)	-0.0173(189)
M_{18}	$2\{\Delta \delta m_{4b} \Delta M_{4b(1^*)} + \Delta L_{4s} \Delta M_{4b} + (\Delta L_{6b1} + \Delta L_{6a2}) M_2\}$	16.9690(39)	17.1897(206)	-0.2207(210)
M_{19}	0	0	0.0002(3)	-0.0002(3)
M_{20}	0	0	0.0010(17)	-0.0010(17)
M_{21}	0	0	0.0003(3)	-0.0003(3)
M_{22}	0	0	-0.0090(25)	0.0090(25)
M_{23}	$2\Delta L_{6h2} M_2$	0.0495(3)	0.0438(59)	0.0057(59)
M_{24}	$2\Delta L_{6g2} M_2$	0.0786(2)	0.0945(61)	-0.0158(61)

20, 21], which is identical with the old approach. For diagrams containing self-energy subdiagrams, however, “gencodeN” treats UV-finite parts of self-energy subdiagrams and IR divergences differently from the old approach [16].

Comparison of the new (*still tentative*) and old calculations has revealed an inconsistency in the treatment of the infrared (IR) divergence in the latter, which is corrected in this letter. Thus we now have two independent evaluations of $A_1^{(8)}$. Of course, much more numerical work is required to reach the precision comparable to that of the old calculation. Fortunately, correction terms themselves can be evaluated easily and very precisely as are shown in (4) and (5).

Finite integrals ΔM_i^{old} , $i = 01, \dots, 47$, from the previous calculation are given in Ref. [10]. ΔM_i^{new} are calculated using the programs generated by “gencodeN” [15, 16]. The numerical values corresponding to $\Delta M_i^{\text{old}} - \Delta M_i^{\text{new}}$ are shown as value B in Tables I and II. Since the diagrams without self-energy subdiagrams do not have IR divergence, ΔM_i^{old} and ΔM_i^{new} should be identical. This is confirmed within the numerical precision of ΔM_i^{new} . On the other hand, diagrams containing self-energy subdiagrams have IR divergence. The new treatment of their contributions produces results different

from those of Ref. [10]. The difference $\Delta M_i^{\text{old}} - \Delta M_i^{\text{new}}$ is listed symbolically in the second column of Tables I and II. Their numerical values are calculated using the lower-order renormalization constants in Table III and are shown as value A in Tables I and II. The difference of value A and value B is listed in the fifth columns of Tables I and II. If both calculations are free from error, value A and value B must agree with each other.

Tables I and II show that “old” and “new” calculations are in good agreement for most diagrams. However, a large discrepancy -0.221 (21) is found for the diagram M_{18} . Though no detectable discrepancy is found for M_{16} , it has a structure similar to M_{18} and is somewhat simpler to analyze. Thus we examine here M_{16} instead of M_{18} .

After an intense scrutiny of the programs of $\Delta M_{16}^{\text{old}}$ and $\Delta M_{16}^{\text{new}}$, our attention was focused on one of the IR subtraction terms of the finite term $\Delta M_{16}^{\text{old}}$ [21, 22]:

$$\begin{aligned}
\Delta M_{16}^{\text{old}} \equiv & M_{16} - \sum_f \prod_{s \in f} \mathbb{K}_s M_{16} \\
& - I_{6c1} M_2 - \frac{1}{2} J_{6c} M_2 - I_{4s} \Delta M_{4a} \\
& - \Delta \delta m_{4a} I_{4b(1^*)} + I_{2^*} \Delta \delta m_{4a} M_2, \quad (3)
\end{aligned}$$

where M_{16} is the bare amplitude, $\sum_f \prod_{s \in f} \mathbb{K}_s M_{16}$ are the UV counter terms defined by the K -operations [15,

TABLE II: Comparison of the numerical calculations of $M_{25} - M_{47}$ of the eighth-order Group V diagrams.

Diagram	difference	value A	value B	$A - B$
M_{25}	0	0	-0.0031(20)	0.0031(20)
M_{26}	$\Delta\delta m_{6f}(M_{2*} - M_{2*}[I])$	2.5114(4)	2.5369(95)	-0.0255(95)
M_{27}	$2\Delta L_{6g4}M_2$	-0.0629(2)	-0.0459(90)	-0.0170(90)
M_{28}	$2\{\Delta\delta m_{6d}(M_{2*} - M_{2*}[I]) + \Delta L_{6c2}M_2\}$	-7.5329(6)	-7.5310(189)	-0.0020(189)
M_{29}	$2\Delta L_{6e2}M_2$	-0.2856(3)	-0.2809(109)	-0.0047(109)
M_{30}	$\Delta\delta m_{6a}(M_{2*} - M_{2*}[I]) + 2\Delta L_{6b2}M_2$	0.2768(7)	0.2490(188)	0.0278(188)
M_{31}	0	0	0.0007(5)	-0.0007(5)
M_{32}	0	0	-0.0024(10)	0.0024(10)
M_{33}	0	0	0.0001(3)	-0.0001(3)
M_{34}	0	0	-0.0010(13)	0.0010(13)
M_{35}	0	0	0.0001(13)	-0.0001(13)
M_{36}	0	0	-0.0027(22)	0.0027(22)
M_{37}	0	0	0.0004(5)	-0.0004(5)
M_{38}	$\Delta\delta m_{6h}(M_{2*} - M_{2*}[I])$	-0.9088(3)	-0.9112(40)	0.0025(40)
M_{39}	0	0	-0.0031(18)	0.0031(18)
M_{40}	$2\Delta\delta m_{6g}(M_{2*} - M_{2*}[I])$	3.8271(6)	3.8326(71)	-0.0055(71)
M_{41}	$\Delta\delta m_{4a}(\Delta M_{4a(2*)}) + \Delta L_{4x}\Delta M_{4a}$	0.9809(3)	0.9713(83)	0.0096(83)
M_{42}	$\Delta\delta m_{6c}(M_{2*} - M_{2*}[I]) + \Delta L_{4l}\Delta M_{4a}$ $+ \Delta\delta m_{4a}\{\Delta M_{4b(2*)} - \Delta\delta m_{2*}(M_{2*} - M_{2*}[I])\}$	-7.0216(5)	-7.0202(114)	-0.0014(114)
M_{43}	$\Delta L_{6h3}M_2$	0.4719(2)	0.4703(42)	0.0016(42)
M_{44}	$2\Delta L_{6g3}M_2$	-0.0751(2)	-0.0499(69)	-0.0253(69)
M_{45}	$\Delta\delta m_{6e}(M_{2*} - M_{2*}[I]) + \Delta L_{6c3}M_2$	-0.0515(6)	-0.0498(90)	-0.0017(90)
M_{46}	$\Delta\delta m_{4b}\Delta M_{4a(2*)} + \Delta L_{6e3}M_2 + \Delta L_{4x}\Delta M_{4b}$	-7.9336(22)	-7.9232(86)	-0.0104(89)
M_{47}	$\Delta\delta m_{6b}(M_{2*} - M_{2*}[I]) + \Delta L_{6b3}M_2 + \Delta L_{4l}\Delta M_{4b}$ $+ \Delta\delta m_{4b}\{\Delta M_{4b(2*)} - \Delta\delta m_{2*}(M_{2*} - M_{2*}[I])\}$	10.5868(15)	10.5864(102)	0.0004(103)

19, 20, 21], and the remainder are the IR subtraction terms. By a term-by-term comparison, we found finally that the IR subtraction term $I_{4b(1*)}$ was the culprit.

Separation of an IR divergent part and a finite part of an integral is arbitrary. However, we must keep track of what is treated as the IR divergent part. In particular the IR subtraction term in ΔM_i and one used to calculate the residual renormalization must be identical. All IR subtraction terms are summed up in the end, which gives a finite contribution as a part of the residual renormalization [21, 22, 23]. What we found is that old FORTRAN codes of $I_{4b(1*)}$ have different forms in ΔM_{16} and in $\Delta M_{4b(1*)}$.

If we use $I_{4b(1*)}$ defined in Ref. [21] as a part of $\Delta M_{4b(1*)}$, we must add the correction term

$$\begin{aligned}\Delta M_{16}^{\text{add}} &\equiv -2 \times \frac{9}{4} \int (dz)_G \frac{\delta m_{4a}[f_0]}{U^2 V^4} \\ &\quad \times z_2 A_2 (1 - A_1)^3 (1 - A_2) \\ &= 0.029\,437\,8 \quad (98)\end{aligned}\quad (4)$$

to $\Delta M_{16}^{\text{old}}$. The functions A_i, U, V in Eq. (4) are defined in the \mathbb{I}_{1237} limit of the diagram M_{16} . For precise definitions of these functions see Refs. [15, 19, 20, 21, 23]. The overall factor 2 comes from the time-reversed diagram. The value (4) is smaller than the uncertainty of value B for M_{16} . Thus it is undetectable by direct comparison of values A and B until precision of $\Delta M_{16}^{\text{new}}$ is improved.

Analyzing the difference of M_{18}^{old} and M_{18}^{new} in the same

manner, we found that the correction term is not small for M_{18} :

$$\begin{aligned}\Delta M_{18}^{\text{add}} &\equiv -2 \times \frac{9}{4} \int (dz)_G (1 - \mathbb{K}_5) \\ &\quad \times \left\{ \frac{\delta m_{4b}[f_0]}{U^2 V^4} z_2 A_2 (1 - A_1)^3 (1 - A_2) \right\} \\ &= -0.215\,542 \quad (19),\end{aligned}\quad (5)$$

where all A_i, U, V are defined in the \mathbb{I}_{1237} limit of M_{18} . Their explicit forms are different from those of M_{16} . The function $\delta m_{4a(b)}[f_0]$ in $M_{16(18)}^{\text{add}}$ is related to the UV-finite part $\Delta\delta m_{4a(b)}$ of the mass-renormalization constant. If we add $\Delta M_{18}^{\text{add}}$ to $\Delta M_{18}^{\text{old}}$, value B of M_{18} becomes 16.974 (21) and the difference between values A and B is reduced to -0.005 (21), which is consistent with zero within the precision of numerical calculation.

We should like to emphasize that the development of automatic code generator [15, 16] was crucial in discovering the existence of extra IR subtraction terms in M_{16} and M_{18} . Details of our investigation will be reported elsewhere [23]. Adding the terms Eq. (4) and Eq. (5) to the “old” calculation Eq. (58) of Ref. [10], we find the entire contribution of Group V:

$$A_1^{(8)}(\text{GroupV}) = -2.179\,16 \quad (343), \quad (6)$$

which is in good agreement with the *still tentative* value obtained by the code generated by “gencodeN”:

$$A_1^{(8)\text{genN}}(\text{GroupV}) = -2.205 \quad (54). \quad (7)$$

TABLE III: Finite renormalization constants used in Tables I and II. The validity of the sixth-order renormalization constants are checked by comparing the sum $X_{LBD} \equiv \sum_{i=1}^5 \Delta L_{6xi} + \frac{1}{2}\Delta B_{6x} + 2\Delta\delta m_{6x}$, $x = a, \dots, h$ to the previous X_{LBD} values listed in Ref. [10].

ΔL_{6a1}	0.539589(67)	ΔL_{6b1}	-1.479347(244)
ΔL_{6a2}	-0.167211(81)	ΔL_{6b2}	0.582944(106)
ΔL_{6a3}	1.489038(142)	ΔL_{6b3}	-0.016344(73)
ΔL_{6c1}	-0.219311(148)	ΔL_{6e1}	-0.740890(373)
ΔL_{6c2}	0.071614(135)	ΔL_{6e2}	-0.285566(252)
ΔL_{6c3}	-0.551410(236)	ΔL_{6e3}	-0.141327(380)
ΔL_{6d1}	0.833454(402)	ΔL_{6g1}	0.088899(251)
ΔL_{6d2}	-0.090653(141)	ΔL_{6g2}	0.078625(184)
ΔL_{6d3}	-0.499683(407)	ΔL_{6g3}	-0.075127(176)
ΔL_{6d4}	-1.377450(287)	ΔL_{6g4}	-0.062906(155)
ΔL_{6d5}	0.694835(227)	ΔL_{6g5}	0.089234(288)
ΔL_{6f1}	-0.006638(212)	ΔL_{6h1}	-0.420233(330)
ΔL_{6f2}	0.080534(139)	ΔL_{6h2}	0.049517(284)
ΔL_{6f3}	-0.226304(227)	ΔL_{6h3}	0.943785(328)
$\Delta\delta m_{6a}$	-0.15309(34)	$\Delta\delta m_{6b}$	1.83775(25)
$\Delta\delta m_{6c}$	-3.05039(22)	$\Delta\delta m_{6d}$	-1.90114(15)
$\Delta\delta m_{6e}$	0.11210(25)	$\Delta\delta m_{6f}$	1.25572(19)
$\Delta\delta m_{6g}$	0.95677(13)	$\Delta\delta m_{6h}$	-0.45439(11)
ΔL_{4c}	0.003387(16)	ΔL_{4x}	-0.481834(54)
ΔL_{4s}	0.407633(20)	ΔL_{4l}	0.124796(67)
$\Delta\delta m_{4a}$	-0.301485(61)	$\Delta\delta m_{4b}$	2.20777(44)
ΔM_{4a}	0.218359(39)	ΔM_{4b}	-0.187526(39)
$\Delta M_{4a(1^*)}$	3.61946(83)	$\Delta M_{4a(2^*)}$	-3.60244(67)
$\Delta M_{4b(1^*)}$	4.25054(23)	$\Delta M_{4b(2^*)}$	1.64475(10)
ΔM_2	0.5	ΔM_{2^*}	1
$\Delta M_{2^*}[I]$	-1	$\Delta\delta m_{2^*}$	-0.75

The revised contribution (6) shifts the total eighth-order term $A_1^{(8)}$ to the one given in Eq. (2). As a consequence, the theoretical prediction of a_e is moved by $-5.421\,775\,(62) \times 10^{-12}$, yielding

$$\begin{aligned} a_e(\text{Rb}) &= 1\,159\,652\,182.78\,(7.72)(0.11)(0.26) \times 10^{-12}, \\ a_e(\text{Cs}) &= 1\,159\,652\,172.98\,(9.33)(0.11)(0.26) \times 10^{-12}, \end{aligned} \quad (8)$$

where 7.72 and 9.33 come from the uncertainties of the input values of the fine structure constant

$$\alpha^{-1}(\text{Rb06}) = 137.035\,998\,84\,(91)\,[6.7\text{ppb}], \quad (9)$$

$$\alpha^{-1}(\text{Cs06}) = 137.036\,000\,00\,(110)\,[8.0\text{ppb}], \quad (10)$$

determined by the Rubidium atom [24] and Cesium atom [25, 26] experiments, respectively. The uncertainty 0.11 of Eq. (8) comes from the eighth-order calculation and 0.26 is an estimated uncertainty of the tenth-order term.

Because of high precision of the experiment (1) the fine structure constant α determined from the theory and the measurement is sensitive to the revision of theory. The inverse fine structure constant $\alpha^{-1}(a_e)$ moves by

$-6.411\,80\,(73) \times 10^{-7}$ from the previous value in Ref. [27]. The revised $\alpha^{-1}(a_e07)$ is about 4.7 ppb (or about 7 s. d.) smaller than $\alpha^{-1}(a_e06)$, but is still in good agreement with $\alpha^{-1}(\text{Rb06})$ of Eq. (9) and $\alpha^{-1}(\text{Cs06})$ of Eq. (10), whose uncertainties are about 7 ppb.

This work is supported in part by the JSPS Grant-in-Aid for Scientific Research (C)19540322. T. K.'s work is supported by the U. S. National Science Foundation under Grant No. PHY-0355005. Numerical calculations were conducted on the RIKEN Super Combined Cluster System(RSCC).

-
- [1] P. Kusch and H. M. Foley, Phys. Rev. **72**, 1256 (1947).
 - [2] J. S. Schwinger, Phys. Rev. **73**, 416 (1948).
 - [3] B. Odom, D. Hanneke, B. D'Urso, and G. Gabrielse, Phys. Rev. Lett. **97**, 030801 (2006).
 - [4] L. S. Brown, G. Gabrielse, K. Helmerson, and J. Tan, Phys. Rev. Lett. **55**, 44 (1985).
 - [5] R. S. Van Dyck, P. B. Schwinberg, and H. G. Dehmelt, Phys. Rev. Lett. **59**, 26 (1987).
 - [6] A. Petermann, Helv. Phys. Acta **30**, 407 (1957).
 - [7] C. M. Sommerfield, Phys. Rev. **107**, 328 (1957).
 - [8] T. Kinoshita, Phys. Rev. Lett. **75**, 4728 (1995).
 - [9] S. Laporta and E. Remiddi, Phys. Lett. **B379**, 283 (1996), hep-ph/9602417.
 - [10] T. Kinoshita and M. Nio, Phys. Rev. D **73**, 013003 (2006), hep-ph/0507249.
 - [11] F. Jegerlehner (1996), private communication.
 - [12] B. Krause (1996), private communication.
 - [13] A. Czarnecki, B. Krause, and W. J. Marciano, Phys. Rev. Lett. **76**, 3267 (1996).
 - [14] P. J. Mohr and B. N. Taylor, Rev. Mod. Phys. **77**, 1 (2005).
 - [15] T. Aoyama, M. Hayakawa, T. Kinoshita, and M. Nio, Nucl. Phys. B **740**, 138 (2006), hep-ph/0512288.
 - [16] T. Aoyama, M. Hayakawa, T. Kinoshita, and M. Nio, in preparation.
 - [17] T. Kinoshita and M. Nio, Phys. Rev. D **73**, 053007 (2006), hep-ph/0512330.
 - [18] G. P. Lepage, J. Comput. Phys. **27**, 192 (1978).
 - [19] P. Cvitanovic and T. Kinoshita, Phys. Rev. D **10**, 3978 (1974).
 - [20] P. Cvitanovic and T. Kinoshita, Phys. Rev. D **10**, 3991 (1974).
 - [21] T. Kinoshita, in *Quantum electrodynamics*, edited by T. Kinoshita (World Scientific, Singapore, 1990), pp. 218–321.
 - [22] T. Kinoshita and W. B. Lindquist, Phys. Rev. D **42**, 636 (1990).
 - [23] T. Aoyama, M. Hayakawa, T. Kinoshita, and M. Nio, in preparation.
 - [24] P. Cladé et al., Phys. Rev. A **74**, 052109 (2006).
 - [25] A. Wicht et al., Phys. Scr. T **102**, 82 (2002).
 - [26] V. Gerginov et al., Phys. Rev. A **73**, 032504 (2006).
 - [27] G. Gabrielse, D. Hanneke, T. Kinoshita, M. Nio, and B. Odom, Phys. Rev. Lett. **97**, 030802 (2006).